Parameter-free one-center model potential for an effective one-electron description of molecular hydrogen

Armin Lühr, Yulian V. Vanne, and Alejandro Saenz
Institut für Physik, AG Moderne Optik, Humboldt-Universität zu Berlin, Hausvogteiplatz 5-7, D-10117 Berlin, Germany
(Received 22 August 2008; published 31 October 2008)

For the description of an H_2 molecule, an effective one-electron model potential is proposed which is fully determined by the exact ionization potential of the H_2 molecule. In order to test the model potential and examine its properties, it is employed to determine excitation energies, transition moments, and oscillator strengths in a range of internuclear distances, $0.8\ \text{a.u.} < R < 2.5\ \text{a.u.}$ In addition, it is used as a description of an H_2 target in calculations of the cross sections for photoionization and for partial excitation in collisions with singly charged ions. The comparison of the results obtained with the model potential with literature data for H_2 molecules yields a good agreement and encourages therefore an extended use of the potential in various other applications or in order to consider the importance of two-electron and anisotropy effects.

DOI: 10.1103/PhysRevA.78.042510 PACS number(s): 31.10.+z, 31.15.B−

I. INTRODUCTION

From the very beginning of quantum mechanics the hydrogen atom has been considered as one of the standard model systems. The reason lies in the simplicity of the theoretical description of this most basic atomic system. On the other hand, the description of the hydrogen molecule is obviously a lot more involved due to the much larger number of degrees of freedom. Compared to the atomic case the complexity of the molecule arises, e.g., from the electron-electron interaction due to the second electron and the anisotropy of the charge distribution, which may lead to an orientational dependence of a physical quantity. Additionally, there is vibrational and rotational motion of the nuclei and even in a Born-Oppenheimer approximation one has to deal with potential curves for all electronic states and their rovibronic excitations.

Consequently, it would be desirable to have a description, although simplified, of the hydrogen molecule at hand which is of similar complexity as the one of the hydrogen atom. This would allow for an easy adoption of already existing numerical methods which were implemented for spherical one-electron problems to the description of molecular hydrogen. But also in complex systems including H_2 molecules like, e.g., H_2 clusters or H_2 adsorbed on surfaces, a simple description of the electronic structure is of interest.

A second motivation becomes even more important in the era of fast improving computational resources, which may make the full description of H_2 molecules feasible even in time-dependent processes. That is, the comparison of results achieved with a full calculation with the outcome of a simplified description of H_2 which has atomic rather than molecular properties and accounts for the second electron only by screening. An analysis of the differences can yield the importance of the influence of two-electron as well as of molecular effects, like the deviation from a spherical symmetric charge distribution.

In the context of the latter motivation a simple one-electron, single-centered model potential was proposed in a recent work [1] which deals with H_2 molecules interacting with short intense laser pulses. Since the strong-field ionization is known to be very sensitive to the electronic binding energy and the exact form of the long-ranged Coulomb potential the proposed model potential is designed to agree in these properties with the H_2 molecule. Thereby, the model potential can be adjusted to an arbitrary internuclear distances by taking the corresponding value of the ionization potential.

Regarding the first motivation, satisfying results have been achieved with the proposed model potential in the description of an H_2 target in collisions with singly charged ions [2]. The calculated total and differential ionization and excitation cross sections agree well with literature data down to projectile velocities for which electron-electron effects may become important. Thereby, also the dependence on the internuclear distance is examined and nuclear motion is taken into account.

The aim of the present work is to further examine the proposed simple single-centered, effective one-electron model potential and to find out why it describes the properties of the hydrogen molecule in the applications [1,2] to different physical systems so well. But also the limits of the model in the description of H_2 molecules should be analyzed. Therefore, quantities like excitation energies, electronic transition moments, and oscillator strengths are calculated as a function of the internuclear distance and are compared to literature data for a full H_2 molecule. Also, the model is used to determine photoionization cross sections and excitation cross sections in collisions with projectiles in order to test its applicability to different physical systems. It may be noted that in the limit $R \to 0$ the model is also suitable for the description of atomic helium, as is shortly commented on in the end.

For a one-electron description of the H_2 molecule also other model potentials exist. To name only three, Teller and Sahlin [3] discussed a two-center approach, while a model potential for He atoms by Hartree [4] was also adjusted to H_2 by fitting it to the correct ionization potential. It can be obtained by integrating an effective hydrogen-atom-like charge distribution with Gauss's theorem. Another widely used model is the scaled hydrogen atom model which treats H_2 as a hydrogen atom with a scaled nuclear charge in order to

achieve the correct ionization potential. The latter model is as simple as the one proposed in [1], but has also the advantage that its wave functions are known analytically. A disadvantage of the scaled potential is, however, that its long-range behavior is not correct. It is therefore used in this work for a comparison of the present results with another H_2 model potential.

The paper is organized as follows: Section II presents the model potential and discusses its properties. Section III considers various applications of the H_2 model: namely, the calculation of excitation energies, transition moments, and oscillator strengths as well as the determination of cross sections for photoionization and excitation in collision processes. Furthermore, the outcome of these applications is discussed and compared to results of experiments and theoretical treatments of the full molecular system. Section IV concludes with the findings. Atomic units are used unless otherwise specified.

II. MODEL POTENTIAL

In order to obtain a simple model for a complex system the right balance has to be found—i.e., a model which reflects the characteristics of the full description. It is known that, e.g., ionization processes of H_2 are very sensitive to the ionization potential I_{H_2} and the properties of the bound states depend on the exact form of the Coulomb potential. Hence, it is important that the model potential agree in these properties with the molecule. An appropriate trade-off for the description of H_2 molecules may be achieved by using the following simple model potential [1] for an effective electron with the radial coordinate r:

$$V_{\mathrm{mod}}(r) = -\left(1 + \frac{\alpha}{|\alpha|}\exp\left[-\frac{2r}{|\alpha|^{1/2}}\right]\right)\Big/ r, \tag{1}$$

where α is a dimensionless term. The model potential satisfies the conditions $V_{\mathrm{mod}}(r) \to -1/r$ for $r \to \infty$ and describes therefore the long-range behavior of an effective H_2 potential correctly as being hydrogen-atom-like. Furthermore, it reduces to the potential of a hydrogen atom H for $\alpha \to 0$ with an ionization potential $I_H = 0.5$ a.u.

The exact dependence of the ionization potential $I_{\mathrm{mod}}(\alpha)$ on α for a system described by V_{mod} can be determined numerically (cf. [1]). However, an advantage of the model proposed in Eq. (1) is the possibility to approximate $I_{\mathrm{mod}}(\alpha)$ quite accurately with the analytic expression

$$I_{\mathrm{mod}}(\alpha) \approx I_H + \alpha \times \begin{cases} (1+\sqrt{|\alpha|})^{-11/4}, & \alpha < 0, \\ (1+\sqrt{|\alpha|})^{-1}, & \alpha \geq 0. \end{cases} \tag{2}$$

For instance, at $R = 1.4$ a.u. the numerically determined ionization potential and $I_{\mathrm{mod}}(\alpha)$ given by Eq. (2) differ only by 0.01%. The dependence on α simplifies even further in the limit $|\alpha| \to 0$, where the ionization potential becomes $I_{\mathrm{mod}}(\alpha) \to I_H + \alpha$ and depends only linearly on α, as can be seen in Table I.

In order to describe an H_2 molecule with a fixed internuclear distance R a certain α has to be determined which fulfills the requirement that $I_{\mathrm{mod}}(\alpha)$ is equal to the ionization potential $I_{H_2}(R)$ of the H_2 molecule at the considered fixed distance R. In Table I values of α which yield the ionization potentials of H_2 for internuclear distances R in a range from 0.8 to 2.5 are given. For a fixed R the ionization potential $I_{H_2}(R)$ is obtained by subtracting the ground-state potential-energy curve of H_2, which was very accurately calculated by Wolniewicz [5] from the ground-state energies of H_2^+. Also given is the α value for the limit $R \to 0$, which yields the correct ionization potential of the helium atom [6].

TABLE I. Values of α used in this work for different internuclear distances R in a.u. The ionization potential $I_{H_2}(R)$ of H_2 for these R is also given in hartrees. It is obtained using the H_2 ground-state potential-energy curve calculated by Wolniewicz [5]. The ionization potential of a He atom [6] and the corresponding α value are also given as the limit $R \to 0$.

R	$\alpha(R)$	$I_{H_2}(R)$
0	0.87910	0.903570
0.8	0.348416	0.715577
0.9	0.302668	0.693373
1.0	0.262548	0.672753
1.1	0.227258	0.653645
1.2	0.196111	0.635961
1.3	0.168525	0.619606
1.4	0.144021	0.604492
1.4487	0.133081	0.597555
1.5	0.122196	0.590531
1.6	0.102722	0.577647
1.7	0.0853182	0.565762
1.8	0.0697585	0.554815
1.9	0.055851	0.544745
2.0	0.0434376	0.535499
2.1	0.0323864	0.527029
2.2	0.0225906	0.519292
2.3	0.0139698	0.512251
2.4	0.00646727	0.505869
2.5	0.00012071	0.500115

Since the model potential can be adopted to different internuclear distances R with the help of α, it is possible to study vibrational effects as was proposed in [7,8]. Ionization cross sections which account for the vibrational motion of the H_2 nuclei in collisions of H_2 targets modeled by V_{mod} with antiprotons were obtained in [2]. They were achieved by employing closure, exploiting the linear behavior of the ionization cross section with R, and performing the calculations at $R = \langle R \rangle = 1.448$ a.u. ($\alpha = 0.133\,08$).

However, a molecule treated in the fixed-nuclei approximation differs from an atom owing to the anisotropy of the electronic charge distribution which cannot be described correctly within an isotropic, single-centered atomic model potential. The effect of anisotropy due to both the two nuclei and due to the second electron in H_2 is to some extent included as a screening of the Coulomb potential. Two-electron effects, like double excitation or double ionization, are naturally not described properly by the model.

In order to compare the properties of the proposed model potential V_{mod} in Eq. (1) with another quite popular (see, e.g., [9]) simple artificial atomic model a scaled hydrogen atom H_{scal} may be introduced. Its potential

$$V_{\mathrm{scal}}(r) = -\frac{Z_{\mathrm{scal}}}{r} \tag{3}$$

differs from a normal H atom due to the scaled nuclear charge Z_{scal}. The correct ionization potential of H_2 at a given R can be obtained for H_{scal} if the nuclear charge is scaled as

$$Z_{\mathrm{scal}}(R) = [I_{H_2}(R)/I_H]^{1/2}. \tag{4}$$

It may be alluded that due to the scaling of the nuclear charge in Eq. (3) all energies ϵ_j of the bound states of H_{scal} are affected in the same way; i.e., they are shifted in comparison to the H atom as

$$\epsilon_j[H_{\mathrm{scal}}] = (Z_{\mathrm{scal}})^2 \epsilon_j[H]. \tag{5}$$

Although the ionization potential of the H_2 molecule is well described by the scaled hydrogen atom, it can be expected that this is not the case for the energies of the bound states, since the potential in Eq. (3) does not have the correct r dependence. Furthermore, one expects problems in the description of molecular properties that are very sensitive to the asymptotic long-range behavior such as tunneling ionization in intense electric or electromagnetic fields.

The physical quantities studied in this work such as oscillator strengths, transition probabilities, or cross sections obtained with an effective one-electron model are multiplied with a factor of 2 in order to account for the two equivalent electrons of H_2. It should be noted that also alternative ways to interpret the results of single-electron models for two-electron systems are possible (e.g., [10]).

III. APPLICATIONS OF THE MODEL POTENTIAL

Since the model potential of Eq. (1) is isotropic, it is naturally qualified for describing orientationally averaged H_2 molecules. This is often the case in experimental studies in which isotropic, nonaligned molecules are investigated. Optical excitations into p states of the model H_2 are consequently compared with both possible dipole-allowed transitions into $^1\Sigma_u$ and $^1\Pi_u$ states of the H_2 molecule. An orientational averaging yields in this case the factors $1/3$ and $2/3$ for a weighting of the results for the symmetries $^1\Sigma_u$ and $^1\Pi_u$, respectively. On the other hand, the isotropy is, of course, a limitation of the model. For example, in the case of multiphoton excitations interference terms prevent a determination of simple weighting factors [1,11].

In what follows, it should be investigated how satisfyingly the proposed model potential works in practice with respect to various applications. First, excitation energies, transition moments, and oscillator strengths are considered. Afterwards, V_{mod} is used for the description of ionization and excitation of an H_2 molecule in interactions with photons and in collisions with particles. The findings are compared to corresponding experimental and theoretical results for an H_2 molecule and partly also to results obtained with H_{scal}.

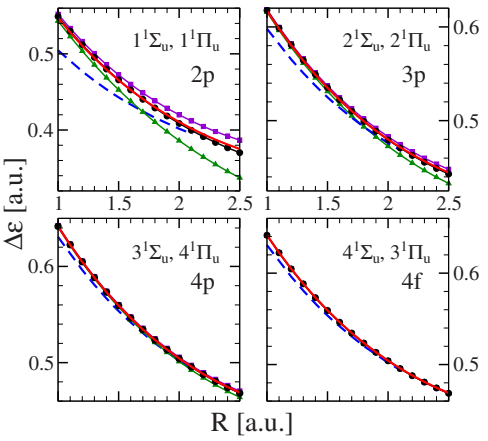

FIG. 1. (Color online) Excitation energies $\Delta\epsilon$ of the H_2 molecule for the four energetically lowest dipole-allowed final states ($n=1,\ldots,4$) for different internuclear distances R calculated by Staszewska and Wolniewicz [12,13]: green triangles, $n^1\Sigma_u$ states; violet squares, $n^1\Pi_u$ states; black circles, orientationally averaged $^1\Sigma_u$ and $^1\Pi_u$ (see text). Present excitation energies for corresponding transitions—i.e., from the ground state to $2p$, $3p$, $4p$, and $4f$: red solid curve, model potential; blue dashed curve, hydrogen atom with scaled nuclear charge H_{scal}.

A. Excitation energies

In Fig. 1 excitation energies (EEs) for the energetically lowest dipole-allowed final states of the H_2 molecule with the symmetries $n^1\Sigma_u$ and $n^1\Pi_u$ with $n=1,\ldots,4$ are given in the range of internuclear distances, 1 a.u. $\leqslant R \leqslant$ 2.5 a.u. They were obtained from the very accurate calculations by Staszewska and Wolniewicz[5,12,13]. The orientationally averaged molecular EEs are given as circles. The corresponding four EEs for an atomic system are the energy differences $\Delta\epsilon$ between the ground state and the $2p$, $3p$, $4p$, and $4f$ states.

It can be seen that in all of the four cases the EE of the model potential approximates the orientationally averaged EE of the H_2 molecule very well in the whole R range considered here. Only for the transition into the $2p$ state are the EEs obtained with the model potential slightly higher than those for H_2 for large R. It is known that in the R range which is considered here the $4^1\Sigma_u$ and $3^1\Pi_u$ states possess a dominant ($1s4f$) contribution [14,15]. Consequently, these states cannot be compared to a p state of the model potential, but instead to the $4f$ state.

In contrast to the findings for V_{mod} the results for the scaled hydrogen atom H_{scal} differ from the other $\Delta\epsilon$ curves especially for small R, while they come close to the correct values for $R>2$ a.u. For large R this trend could have been expected since the H_2 molecule becomes more and more like two distant H atoms and therefore can be modeled by the hydrogen-atom-like H_{scal}. However, it is known that, e.g., the excitation probability can depend considerably on the EE [16] and therefore should be described accurately, especially around the equilibrium distance $R \approx 1.4$ a.u.

B. Electronic transition matrix elements

Another test of the capability of the model potential V_{mod} given in Eq. (1) can be performed by considering transition

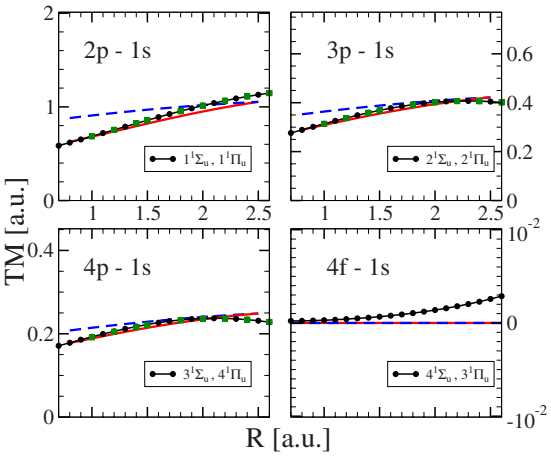

FIG. 2. (Color online) Electronic TMs of the H_2 molecule as a function of R for transitions from the ground state $1\,^1\Sigma_g$ to the four orientationally averaged, energetically lowest, dipole-allowed final states consisting of the symmetries $^1\Sigma_u$ and $^1\Pi_u$: black circles, Wolniewicz and Staszewska [13,14]; green squares, Drira [17]. Present results for corresponding transition moments—i.e., from the ground state to $2p$, $3p$, $4p$, and $4f$: red solid curve, model potential V_{mod}; blue dashed curve, hydrogen atom with scaled nuclear charge H_{scal}. (Note the different scales, especially for the $4f$-$1s$ transition.)

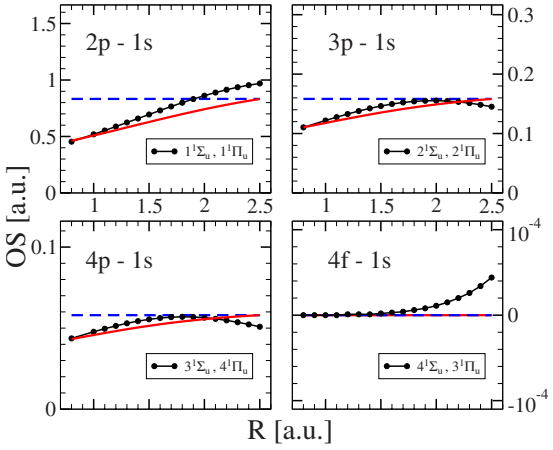

FIG. 3. (Color online) OSs of the H_2 molecule as a function of R for transitions from the ground state $1\,^1\Sigma_g$ to the four orientationally averaged, energetically lowest, dipole-allowed final states consisting of the symmetries $^1\Sigma_u$ and $^1\Pi_u$: black circles, Wolniewicz and Staszewska [12,14,13]. Results for corresponding transition moments—i.e., from the ground state to $2p$, $3p$, $4p$, and $4f$: red solid curve, present; blue dashed curve, hydrogen atom with scaled nuclear charge H_{scal}.

moments (TMs), which are known to be much more sensitive to the behavior of the wave functions than the energies. The dipole TMs into the state $|nl\rangle$ for a fixed R,

$$M(nl) = \sqrt{2}\langle 1s|\hat{\mathbf{x}}|nl\rangle, \tag{6}$$

were computed for the same transitions which have been already discussed in Sec. III A, where n and l are the principal and angular momentum quantum numbers, respectively. The factor of $\sqrt{2}$ in Eq. (6) accounts for the two electrons in the H_2 molecule. TMs from the H_2 ground state $1\,^1\Sigma_g$ to the dipole-allowed final states $^1\Sigma_u$ and $^1\Pi_u$ were calculated by Wolniewicz and Staszewska [13,14], Spielfiedel [15], and Drira [17]. In Fig. 2 the orientationally averaged molecular TMs are compared to the present results obtained with the model potential, whereas the wrong assignment done in [17] for molecular states with dominant $(1s4p)$ or $(1s4f)$ configuration is corrected as proposed in [13–15]. Also given are the TMs for the scaled hydrogen atom H_{scal}.

In general, the present TMs achieved with V_{mod} agree with the data for the full H_2 molecule. For $R > 1.5$ a.u. there is some deviation for the transition into the $2p$ state which could have been expected, since the electron-electron interaction and the effects due to the two nuclei are most prominent for the lowest excited states. Otherwise, all TMs to higher states match the literature data very well. It may be noted that even the molecular states $4\,^1\Sigma_u$ and $3\,^1\Pi_u$—both with dominant $(1s4f)$ character at small R—are again nicely represented by the non-dipole-allowed $4f$ state of the model. The EEs as well as the vanishing TMs of the $4f$ state match the corresponding orientationally averaged results of the H_2 molecule.

The TMs calculated for H_{scal} show for all p transitions a different dependence on R than the TMs for H_2. For small R they are too large, and for $R \to 2.5$ a.u. they approach the TMs calculated for V_{mod}. The deviations indicate that, especially at small R, the properties of the wave functions obtained with V_{scal} differ considerably from those of a real H_2 molecule.

C. Oscillator strengths

Figure 3 shows the oscillator strengths (OSs) of the H_2 molecule, the model potential V_{mod}, and H_{scal} as a function of R for the same transitions which were already considered before. It may be argued that the procedure of orientational averaging is most appropriate for the OS since they obey the Thomas-Reiche-Kuhn sum rule. Since the OSs depend on the EEs and TMs, the question is whether this leads to a compensation or even to an increase of the deviations between model and real molecule. The OSs from the ground into the excited state $|nl\rangle$ are given by

$$f(nl) = \frac{2}{3}(\epsilon_{nl} - \epsilon_0)|M(nl)|^2, \tag{7}$$

where ϵ_0 and ϵ_{nl} are the energies of the ground and final excited states $|nl\rangle$, respectively. The OSs for the H_2 molecule are constructed in the same way using the data calculated by Wolniewicz and Staszewska [12–14]. First, the OSs for both symmetries $^1\Sigma_u$ and $^1\Pi_u$ were determined separately and afterwards orientationally weighted with factors of $1/3$ and $2/3$, respectively, in order to compare to the present results.

It can be seen in Fig. 3 that the OSs of H_{scal} are independent of R and are therefore the same as for the hydrogen atom. This is due to a cancellation of the Z_{scal} dependence in Eq. (7). Therein the dependence on Z_{scal} of the energies is $\epsilon \propto (Z_{\mathrm{scal}})^2$ [cf. Eq. (5)] and of the TMs is $M \propto 1/(Z_{\mathrm{scal}})$. It is even necessary that the OSs of H_{scal} are independent of R since a scaling of the OSs with a single factor would lead to

a violation of the above-mentioned sum rule.

The OSs of the H_2 molecule and for V_{mod} are, however, not independent of the internuclear distance R. For all transitions the OSs of H_2 and the present model agree well for small R. For increasing R the OSs obtained with V_{mod} increase roughly linearly, while those for H_2 show a different behavior for $R>1.5$ a.u. However, the magnitudes are still comparable. At $R=2.5$ a.u. the OSs obtained with V_{mod} and V_{scal} coincide, which already could have been expected before from the results for the related EEs and TMs. For this distance both potentials become hydrogen-atom-like. Considering the region around $R=1.4$ a.u.—which is most important for many calculations with fixed R considering processes starting from the H_2 ground state—one can conclude that the OSs of the H_2 molecule are satisfyingly modeled by the proposed potential V_{mod}.

D. Photoionization cross sections

A calculation of the photoionization spectrum for the hydrogen molecule is used to demonstrate the applicability of the present model to interaction processes in which an H_2 molecule is ionized. In doing so, the representation of the continuum states is probed. Further applications of V_{mod} in order to describe ionization of H_2 in time-dependent processes can be found elsewhere [1,2]. The photoionization cross section is given by

$$\sigma_{ph}(\epsilon) = \frac{4\pi^2}{c}(\epsilon - \epsilon_0)|M(\epsilon)|^2\rho(\epsilon), \tag{8}$$

where ϵ is the positive energy of the ionized final state $|\epsilon\rangle$ with an angular momentum $l=1$ and c is the speed of light. The transition matrix elements $M(\epsilon)$ are defined in the same way as in Eq. (6) except that the $|\epsilon\rangle$ are considered as final states. The density of continuum states $\rho(\epsilon)$ is used for energy normalization of the cross section.

The present photoionization cross sections were calculated for $R=1.4$ a.u. in order to compare the results with theoretical calculations from the literature in which the fixed-nuclei approximation was used. Besides the theoretical results by Sánchez and Martín [18], also experimental photoionization cross sections are shown in Fig. 4, which were measured by Lee *et al.* [19], Chung *et al.* [20], and Latimer *et al.* [21].

It can be seen that the experimental photoionization cross sections are well described by the present model. At low energies, however, the results by Chung *et al.* and Lee *et al.* lie slightly above and below the present curve, respectively. The measurements by Latimer *et al.* where performed between approximately 0.9 and 1.3 a.u. on a dense energy grid searching for resonances above 1.1 a.u., which they did not find. Their data match very well with the present curve, which is, of course, free of any resonance caused by doubly excited states. The clearly visible resonances in the theoretical data calculated by Sánchez and Martín around $R=1.12$ and 1.25 a.u. were explained by Martín [22] as being only visible within the fixed-nuclei approximation. In a further calculation which includes nuclear motion [22] the resonance effects are, in accordance with experimental results, practically invisible. This was explained by the broadening of the resonances, if the nuclear degrees of freedom are included. For energies below 1.1 a.u. where no resonances occur in the data of [18] their calculation agrees well with the present curve.

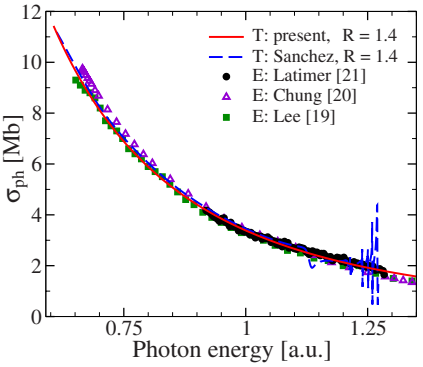

FIG. 4. (Color online) Total photoionization cross section of H_2 as a function of the photon energy for a fixed internuclear distance $R=1.4$ a.u. Theory: red solid curve, present results with model potential; blue dashed curve, Sánchez and Martín [18]. Experiment: green squares, Lee *et al.* [19]; violet triangles, Chung *et al.* [20]; black circles, Latimer *et al.* [21].

E. Collisional excitation cross sections

While the ionization probability depends strongly on the ionization potential, the excitation process is more sensitive to bound-state properties. Therefore, a calculation of an excitation cross section for the H_2 molecule is used to demonstrate that the model potential is also capable to describe transitions to bound states properly.

In Fig. 5 the partial cross section for the energetically lowest dipole-allowed transition for H_2 collisions with pro-

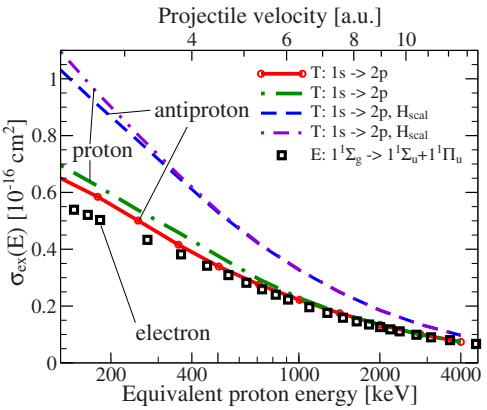

FIG. 5. (Color online) Differential cross sections σ_{ex} for excitation into the lowest dipole-allowed states of H_2 as a function of the projectile velocity v in a.u. and of the equivalent proton energy E in keV. Theory: present results for a fixed internuclear distance $R=1.4$ a.u. for excitation into $2p$. Model potential V_{mod}: red solid curve, antiprotons; green dash-dotted curve, protons. H_{scal}: blue dashed curve, antiprotons; violet dash-double-dotted curve, protons. Experiment: sum of cross sections for excitations into $1^1\Sigma_u$ and $1^1\Pi_u$: black squares, electrons, Liu *et al.* [23].

tons and antiprotons is shown where the H_2 target is described with the model potential. Detailed information concerning the employed time-dependent method is given elsewhere [2]. This transition has been chosen since, first, it is the most probable excitation in this energy range and, second, in Secs. III B and III C the largest deviation of the TMs and OSs between the model and the H_2 molecule have been observed for this transition. Furthermore, partial cross sections can be used for a more sensitive testing because the errors of total cross sections may be reduced by some error compensation. The present results are compared with experimental data for H_2 collisions with electrons measured at a temperature of 10 K by Liu *et al.* [23] due to the fact that to the best of the authors' knowledge no measurements have been performed for proton or antiproton impact. In addition, also results for proton and antiproton collisions with H_{scal} are given in Fig. 5.

The results for protons and antiprotons obtained with the proposed model potential V_{mod} coincide for large impact energies $E>1000$ keV as is expected. At these high energies they also fully agree with the experimental data for electrons with the same impact velocity v. This behavior at high impact velocities is predicted by the first Born approximation; i.e., the same cross section can be expected for collisions including particles with the same absolute value of the charge and the same impact velocity. At smaller energies the cross sections start to depend on the properties of the projectile. Thereby, the antiproton results are closer to the measured electron data than the results for proton impact since the former both share the same charge [24].

The H_{scal} results for protons and antiprotons also coincide for high impact energies as expected in the first Born limit. However, the excitation cross sections for H_{scal} in Fig. 5 as well as in [2] clearly show a different behavior than the experimental data and the results obtained with the potential V_{mod}.

In contrast to the present results, the use of H_{scal} as a target model in calculations of total ionization cross sections of an H_2 molecule can yield to a certain extent reasonable results [2]. The mixed capability of H_{scal} in describing the H_2 molecule may be explained in the following way. On the one hand, concerning ionization, the ionization potential is in both models—i.e., V_{mod} and V_{scal}—by definition correct. On the other hand, the potentials differ in their r dependence and the short-range as well as the long-range behavior of V_{scal} obviously disagrees with that of an H_2 molecule. This leads to a poor description of the bound states and finally to wrong excitation cross sections. This is in accordance with the deviations of the OSs in Fig. 3, which indicate too large excitation probability for H_{scal} at $R=1.4$ a.u.

F. Helium atom

In the limit $R\rightarrow 0$ with $\alpha=0.8791$ the model potential V_{mod} can be used for the description of a helium atom. Obviously, various different one-electron potentials have already been proposed in order to describe He atoms. There are, e.g., the well-known Thomas-Fermi and Hartree models as well as the Hartree-Fock-Slater (HFS) model [25], which includes a local exchange correction and was applied, e.g., in [26]. Another approach is the optimized potential method (OPM) discussed in [27,28] which was used to calculated p+He loss cross sections in [29].

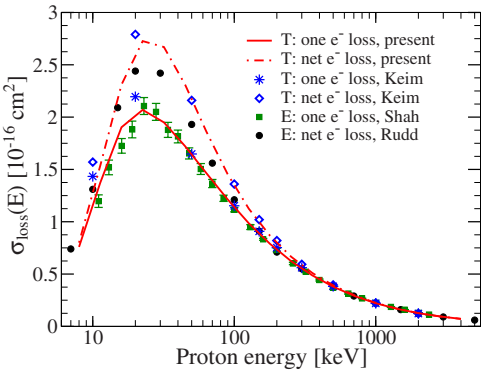

FIG. 6. (Color online) Electron-loss cross section of He collisions with protons. One-electron loss. Theory: red solid curve, V_{mod} with $\alpha=0.8791$; blue stars, Keim *et al.* [29]. Experiment: green squares, Shah *et al.* [30,31]. Net electron loss. Theory: red dash-dotted curve, V_{mod} with $\alpha=0.8791$; blue diamonds, Keim *et al.* [29]. Experiment: black circles, Rudd *et al.* [32].

In Fig. 6 electron-loss cross sections (the sum of ionization and capture) are shown for collisions of protons with He atoms. The present results were obtained with the same method which was employed for the p and $\bar{p}$ collisions with H_2 in Sec. III E and which was discussed in detail in [2,16]. Measurements of the one-electron loss were performed by Shah *et al.* [30,31]. Cross sections for the net electron loss were experimentally determined by Rudd *et al.* [32]. Calculations of the one-electron and net electron loss were done by Keim *et al.* [29] using the OPM with a time-independent effective potential.

In the present results for the net electron loss the probabilities for double capture, double ionization, and transfer ionization are counted twice in order to get the correct number of electrons lost in the collision process. All theoretical data points for the net electron loss by Keim *et al.* coincide fully with the present findings apart from those for the two lowest impact energies (10 and 20 keV), which are clearly higher than the present ones. The present net-loss cross sections reproduce the experimental data by Rudd *et al.* to a great extent. However, in the energy range 20 keV$<E<100$ keV the experimental data are smaller than the outcome of both theoretical investigations.

In the case of the one-electron loss the present findings match the experimental results by Shah *et al.* well in the whole impact energy range of the protons. Again all theoretical data points by Keim *et al.* coincide fully with the present ones besides those for the two lowest impact energies, which have again larger values. Finally, it can be concluded that in addition to H_2 the proposed model potential V_{mpd} is also capable of a simple description of He atoms which is consistent with the OPM without response.

IV. CONCLUSION

A simple model potential V_{mod} for an effective one-electron, single-centered description of the H_2 molecule has

been proposed, and its properties have been examined. The potential is unambiguously determined by the correct ionization potential of the H_2 molecule and allows for the description of H_2 at an arbitrary internuclear distance R. Thereby, also the nuclear motion can be considered to some extent.

The model potential was used for various applications in the range $0.8\ \text{a.u.} \leqslant R \leqslant 2.5\ \text{a.u.}$ The energetically lowest dipole-allowed excitation energies and transition moments as well as oscillator strengths of the H_2 molecule are represented well by the present model. The model was furthermore employed for the calculation of the photoionization cross section of H_2 and a partial excitation cross section in collisions of H_2 with charged particles. In both applications experimental and also theoretical literature data could be well described by the present results obtained with the model potential.

Concerning the scaled hydrogen atom as model for H_2 the results for ionization are satisfying, while bound states properties and therefore also excitation cross sections are not reproduced adequately.

The satisfying description of results for H_2 molecules justifies, on the one hand, the choice of the ionization potential of H_2 as a criterion for adjusting V_{mod} to a certain internuclear distance. On the other hand, together with the surpassing simplicity of the model which includes an approximate analytic expression for the ionization potential, it suggests its applicability to a large number of further problems. To name only some, there are, e.g., the description of the electronic structure of H_2 molecules in H_2 clusters, H_2 molecules interacting with external fields or with particles, and finally also the modeling of He atoms in the limit $R \to 0$.

It can be concluded that the H_2 molecule is in many cases surprisingly well described by a single-electron, one-center model. This means that in these cases the effects of charge anisotropy and two-electron effects are small.

ACKNOWLEDGMENTS

The authors wish to thank H. J. Lüdde for a discussion on effective one-electron models. The authors also would like to thank F. Martín and T. Kirchner for providing cross sections in numerical form. The authors are grateful to BMBF (FLAIR Horizon), DFG, and "Stifterverband für die deutsche Wissenschaft" for financial support.

[1] Y. V. Vanne and A. Saenz, J. Mod. Opt. **55**, 2665 (2008).
[2] A. Lühr and A. Saenz, Phys. Rev. A **78**, 032708 (2008).
[3] E. Teller and H. L. Sahlin, in *Valency*, Vol. 5 of *Physical Chemistry: An advanced tratise*, edited by H. Eyring (Academic Press, New York, 1970), Sec. 2.C.
[4] D. R. Hartree, *The Calculation of Atomic Structures* (Wiley, New York, 1957), Sec. 2.E.
[5] L. Wolniewicz, J. Chem. Phys. **99**, 1851 (1993).
[6] NIST (National Institue of Standards and Technology), http://physics.nist.gov/PhysRefData/ASD/index.html
[7] A. Saenz and P. Froelich, Phys. Rev. C **56**, 2162 (1997).
[8] L. F. Errea, J. D. Gorfinkiel, A. Macías, L. Méndez, and A. Riera, J. Phys. B **30**, 3855 (1997).
[9] A. M. Ermolaev, Hyperfine Interact. **76**, 335 (1993).
[10] Y. D. Wang, C. D. Lin, N. Toshima, and Z. Chen, Phys. Rev. A **52**, 2852 (1995).
[11] A. Apalategui and A. Saenz, J. Phys. B **35**, 1909 (2002).
[12] G. Staszewska and L. Wolniewicz, J. Mol. Spectrosc. **212**, 208 (2002).
[13] L. Wolniewicz and G. Staszewska, J. Mol. Spectrosc. **220**, 45 (2003).
[14] L. Wolniewicz and G. Staszewska, J. Mol. Spectrosc. **217**, 181 (2003).
[15] A. Spielfiedel, J. Mol. Spectrosc. **217**, 162 (2003).
[16] A. Lühr and A. Saenz, Phys. Rev. A **77**, 052713 (2008).
[17] I. Drira, J. Mol. Spectrosc. **198**, 52 (1999).
[18] I. Sánchez and F. Martín, J. Phys. B **30**, 679 (1997).
[19] L. C. Lee, R. W. Carlson, and D. L. Judge, J. Quant. Spectrosc. Radiat. Transf. **16**, 873 (1976).
[20] Y. M. Chung, E.-M. Lee, T. Masuoka, and J. A. R. Samson, J. Chem. Phys. **99**, 885 (1993).
[21] C. J. Latimer, K. F. Dunn, F. P. O'Neill, M. A. MacDonald, and N. Kouchi, J. Chem. Phys. **102**, 722 (1995).
[22] F. Martín, J. Phys. B **32**, R197 (1999).
[23] X. Liu, D. E. Shemansky, S. M. Ahmed, G. K. James, and J. M. Ajello, J. Geophys. Res., [Space Phys.] **103**, 26739 (1998).
[24] H. Knudsen and J. F. Reading, Phys. Rep. **212**, 107 (1992).
[25] J. C. Slater, Phys. Rev. **81**, 385 (1951).
[26] L. Gulyás, P. D. Fainstein, and A. Salin, J. Phys. B **28**, 245 (1995).
[27] T. Kirchner, L. Gulyás, H. J. Lüdde, A. Henne, E. Engel, and R. M. Dreizler, Phys. Rev. Lett. **79**, 1658 (1997).
[28] J. D. T. K. Aashamar and T. M. Luke, At. Data Nucl. Data Tables **22**, 443, (1978).
[29] M. Keim, A. Achenbach, H. J. Lüdde, and T. Kirchner, Nucl. Instrum. Methods Phys. Res. B **233**, 240 (2005); M. Keim, Ph.D. thesis, Universität Frankfurt, Germany, 2005.
[30] M. B. Shah and H. B. Gilbody, J. Phys. B **18**, 899 (1985).
[31] M. B. Shah, P. McCallion, and H. B. Gilbody, J. Phys. B **22**, 3037 (1989).
[32] M. E. Rudd, R. D. DuBois, L. H. Toburen, C. A. Ratcliffe, and T. V. Goffe, Phys. Rev. A **28**, 3244 (1983).